



# Investigation of the Effect of Solidification Time and Addition Amount of Inoculation on Microstructure and Hardness in Lamellar Graphite Cast Iron

M. Çolak <sup>a,\*</sup>, E. Uslu <sup>a</sup>, Ç. Teke <sup>a</sup>, F. Şafak <sup>b</sup>, Ö. Erol <sup>b</sup>, Y. Erol <sup>b</sup>, Y. Çoban <sup>b</sup>, M. Yavuz <sup>c</sup>

<sup>a</sup> Bayburt University, Turkey

<sup>b</sup> Konya Technical University, Turkey

<sup>c</sup> Yavuzsan A.Ş., Turkey

\* Corresponding author. E-mail address: mcolak@bayburt.edu.tr

Received 15.06.2022; accepted in revised form 14.09.2022; available online 25.11.2022

## Abstract

Material suppliers typically recommend different additive amounts and applications for foundry practices. Therefore, even in the production of the same standard materials, different results may be obtained from various production processes on different foundry floors. In this study, the liquid metal prepared with the addition of different proportions of a FeSi-based inoculation, which is most commonly used in foundries in the production of a cast iron material with EN-GJL-250 lamellar graphite cast iron, was cast into sand molds prepared with a model designed to provide different solidification times. In this way, the optimization of the inoculation amounts on the casting structure for different solidification times was investigated. In addition, hardness values were determined depending on solidification time in varying amounts of inoculation additions. SolidCast casting simulation software was used to determine the casting model geometry and solidification time. In the scope of the study, sand casting, modeling, microstructure analysis, image analysis, microstructure analysis, and hardness tests techniques were used. When the results are examined, the required amount of inoculation for the optimal structure is optimized for the application procedure depending on the casting module and the solidification time.

**Keywords:** Lamellar graphite cast iron, Inoculation, Solidification time, Modeling

## 1. Introduction

Cast irons have a wide range of strength, hardness, corrosion resistance, easy workability, wear resistance, and vibration damping properties. Despite the intense competition from new materials, cast irons are still in demand as a suitable and economical material in thousands of engineering applications [1].

In cast iron, most of the carbon content decomposes during solidification and is seen as a separate structural element in the microstructure. The shape and form of the carbon determine the type of cast iron and therefore the properties [2-4]. In cast iron, the fact that the graphite shape is lamellar, spherical, or compact also leads to a different strength, ductility, and shrinkage porosity [5]. The formation of a phase of low-density graphite during solidification increases the volume of cast iron due to the expansion



of the phase, and the resulting pressure can help eliminate the microporosity of the shrinkage in casting [6]. During slow cooling of the cast iron, the carbon is transformed into lamellar shape graphite in the presence of high carbon and silicon, thereby it is known as lamellar graphite cast iron. The microstructure depends on the cooling rate, alloying elements, casting temperature, spheroidization, and inoculation processes. According to Skaland et al. [7], the morphology of graphite depends on the inoculation that is used during treatment. A different study by Rowley [8] also stated that each graphite in cast iron should be nucleated during solidification, and effective inoculation is essential to obtain the desired microstructure. As much as the mechanical properties are affected by the microstructure, the presence of defects is also critical. In cast iron, the main defects that adversely affect the material properties are associated with the shape and dimensions of the graphite particles particularly in the thick sections, in the thermal center of the castings, where solidification takes longer. Shrinkage porosity or inclusions are other harmful defects that reduce mechanical resistance [9,10]. Microstructure and defects can be checked with special inoculation treatments as appropriate. In one study, the authors showed how inoculation with rare earth metals and bismuth significantly reduced the formation of large graphite in thick-section ductile iron castings [11]. Skaland [12] emphasized that the control of chemical composition and process parameters is essential in obtaining sound castings. In particular, high lamellar and nodule counts, which prevent the formation of shrinkage porosities, can be achieved by optimizing the inoculation process [12]. In a different study, Colak [13] found that it is possible to reduce micro-porosity shrinkage with an improvement in fatigue resistance with optimization of the inoculation process and a decrease in the scattering band in fatigue test results. It is known that inoculants are also effective in the fluidity of cast irons [14]. The development of casting properties by processes such as inoculation, and alloying element additions during the production stages with cast iron is one of the commonly used applications.

Inoculation is added to liquid metal to ensure controlled graphite structure, which increases mechanical properties by reducing carbide formation, reproducing eutectic structure, decrystallization, and growth of graphite by providing nuclearization, and ensuring compatibility between casting parts at different cross-section changes [15-16]. As the number of nuclei increases with the aid of inoculation in cast irons, carbon atoms will not find the time to diffuse longer distances, and thereby finely distributed graphite is formed in the structure [15]. Since it increases the uniformity of the cast-iron structure, the inoculation process is critical, and it helps to eliminate the formation of carbides [17]. In addition, the inoculation process facilitates the transformation of cast graphite structures from type D to type A eutectic structures [18]. Increasing the number of nuclei during inoculation generates a heat flow which helps homogeneous cooling of the cast part [18-21]. At what rate the inoculation will be added depends on a large number of variables. It is possible to consider the main variables as liquid metal composition, casting temperature, part thickness, mold material, melting condition, and casting time. The size of the inoculation material should be small enough to melt quickly and large enough so that it does not oxidize immediately and does not burst suddenly. In generalization, inoculation is required as late as possible to get a good result; the effect of inoculation disappears with time. This time leads to heat

loss, and the decreasing heat also reduces the number of graphite spheres. In addition, the higher the inoculation temperature, the lower the inoculation efficiency. Therefore, it is most convenient to inoculate at the lowest possible temperature and the last moment [22]. The most widely used inoculants are ferrosilicon, which contains a small number of elements such as Al, Ba, Ca, Sr and Zr. The most well-known are those that have 50%-80% rates. These alloys mainly contain calcium. The addition of the inoculator can be carried out in the furnace, in the crucible, in the stream, or the mold [23]. The success of inoculation depends on two main factors. These are the quality and quantity of the inoculator added to the liquid metal quality. At what rate the inoculation will be added depends on a large number of variables. The main variables are liquid metal composition, casting temperature, part thickness, mold material, melting condition, and casting time. Therefore, a large number of variables make it impossible to determine a constant inoculation rate. Increasing the amount of 75% FeTi inoculants increases the amount of graphite [24-27]. It is known that inoculants are more effective when the cross-sectional thickness increases [28]. Using various inoculants in different proportions in the production of cast iron GJL-casting material and the experiments in this study, 60 microstructure and mechanical properties of the produced material were investigated and the finer the grain size, the grain size of the samples used in the inoculant used samples revealed superior mechanical properties compared to the large. In addition, a decrease in hardness was detected with the addition of inoculants. In the study, it was determined that the shape of the graphite spheres formed in the structure after the addition of the inoculator was appropriate, the diameter of the sphere was, on average, about 15  $\mu\text{m}$ , and the number of spheres per  $\text{mm}^2$  was within the required values in the standards [29]. In a study conducted comparing the actual castings and modeling of gray cast irons, it was observed that the thickness of the lamella changed from a change in the cooling rate depending on the thickness of the section in microstructure studies. Since solidification will be completed later in regions with thick sections, the graphite structure will have time to grow, and it has been found that coarser structures are formed [30].

In this study, castings were made into a mold prepared with a model containing a different solidification time with the addition of various amounts of inoculator in the production of an EN-GJL-250 cast iron material with lamellar graphite structure. Microstructure and hardness studies of the cast samples were carried out to determine the optimum amount of inoculant with regard to the change in solidification time at different section thicknesses.

## 2. Material and method

The geometry and dimension of the mould used in this study are given in Figure 1. The castings were made with EN-GJL-250 lamellar graphite cast iron material. The part used in casting experiments is designed to have different solidification times with regard to the different section thickness. The model was molded horizontally in casting studies, and the feeder design was made in the SolidCast casting simulation program. The required cylindrical riser dimensions were determined from modeling studies, which should have a diameter of 40 mm and a height of 60 mm. In

addition, it has been determined that the gate should have a rectangular section of 5 x 15 mm to ensure that the part comes out intact during volumetric expansion during solidification.

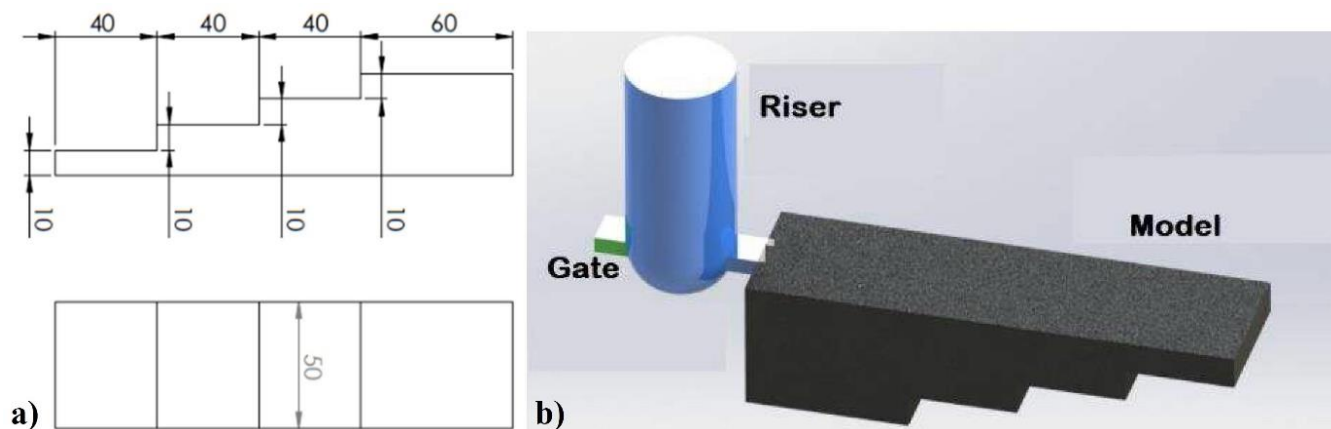


Fig. 1. a) geometry and dimension of the cast part, b) solid model image

Alpha set resin sand was used for the preparation of molds. 1.5 kg resin and 1 kg agent were added to 100 kg sand. After the mold was prepared, the molds were prepared by curing in the air. The melting and casting processes were carried out in an induction furnace at the commercial foundry. The inoculation process was applied in two stages: (i) at the transfer ladle and (ii) at the mold during pouring. Calcium-based inoculation was used while transferring 70% of the total amount of inoculant from the furnace to the crucible. The remaining 30% inoculant was made using barium-based inoculation during crucible-to-mold casting. After pouring 20-25% of the liquid metal into the mold, the inoculant was added to the liquid metal at the entrance of the mold. Afterward, the application was carried out by providing a fixed amount until 75-80% of the mold was filled. A similar application was made during the removal of liquid metal from the furnace to the crucible. After removing the cast parts from the mold, they were separated from the runners and feeders and subjected to inspections.

After the castings were complete, the samples were subjected to metallographic preparation processes for microstructure studies,

and their evaluation was carried out with the image analysis. The samples were first ground with 180, 400, 600, 800, 1000, and 1200 SiC grit papers. After that, it was subjected to polishing with 6  $\mu\text{m}$  and 3  $\mu\text{m}$  diamond solution. Microstructure examinations were made on a Nikon Eclipse L150-A type microscope. Using Clemex Vision Lite image analysis software was used for the analysis. In microstructure image analysis studies, lamellar thickness, length, phase distribution, and phase ratio were determined. Measurements for Brinell hardness tests of the samples were carried out at room temperature with the STRUERS Duramin-500 hardness device.

### 3. Results

The chemical composition analysis result of the alloy used in the experiments is given in Table 1. The chemical composition values are found to be within the standard composition range of EN-GJL-250 alloy.

Table 1.

Chemical composition of the EN-GJL-250 casting alloy used in the experiments

Element	C	Si	Mn	P	S	Cr	Mo	Ni	Cu	Mg
%	3.61	1.78	0.49	0.041	0.035	0.054	0.016	0.036	0.151	0.001

#### 3.1. Modeling results and determination of solidification time

Simulation studies were carried out using SolidCast according to the design given in Figure 1. When the results were examined, there was no macro and microporosity on the part as seen in Figure 2.

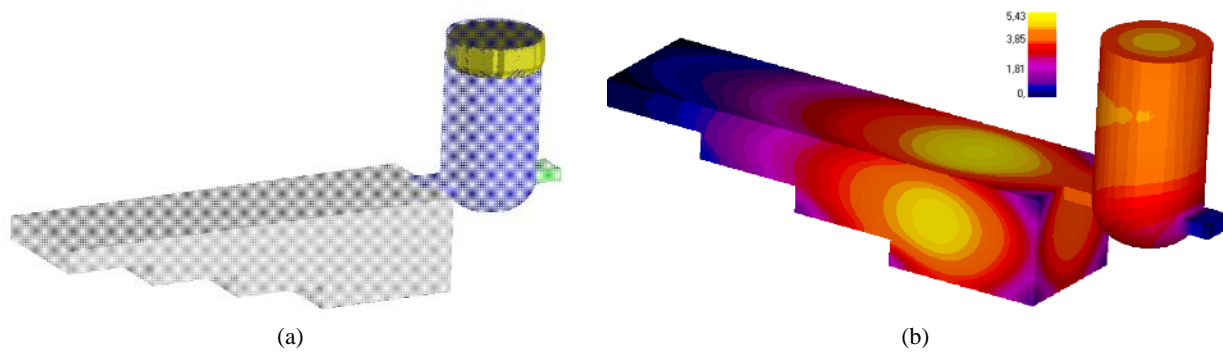


Fig. 2 Simulation results for a) Macroporosity shrinkage analysis, b) solidification time

Modulus analysis values for the design used in the tests are given in Figure 3. It has been determined that the module value is between 0.26 and 0.97 cm for different thicknesses.

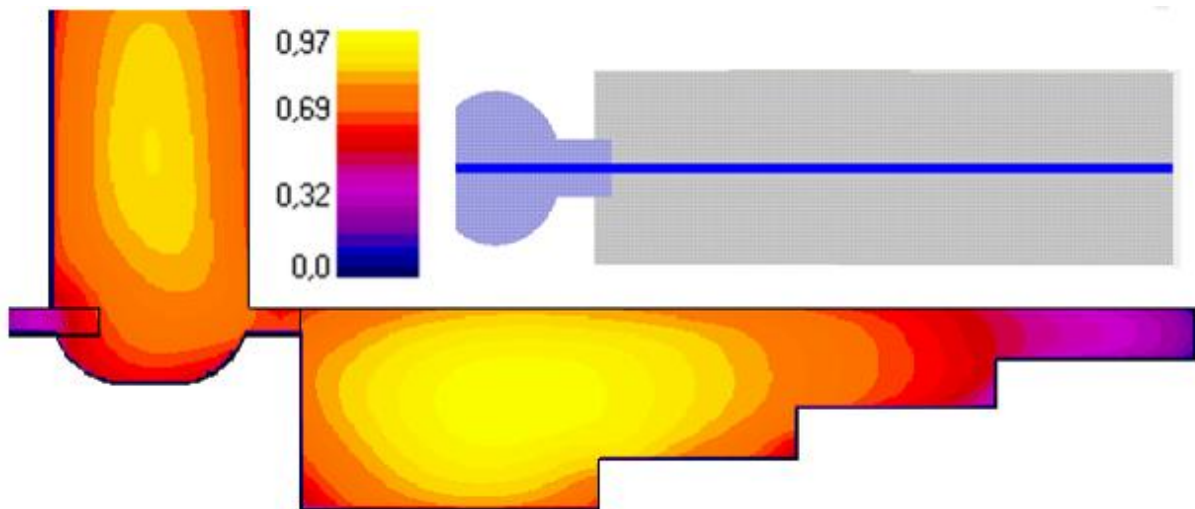


Fig. 3. Modulus values of each thickness

The regions where the solidification time values are taken from the simulation and the solidification time in minutes are given in Figure 4. As can be seen, it is understood that the solidification of the part

starts from 0.2 minutes in the thinnest section and continues up to 5.438 minutes in the thickest area.

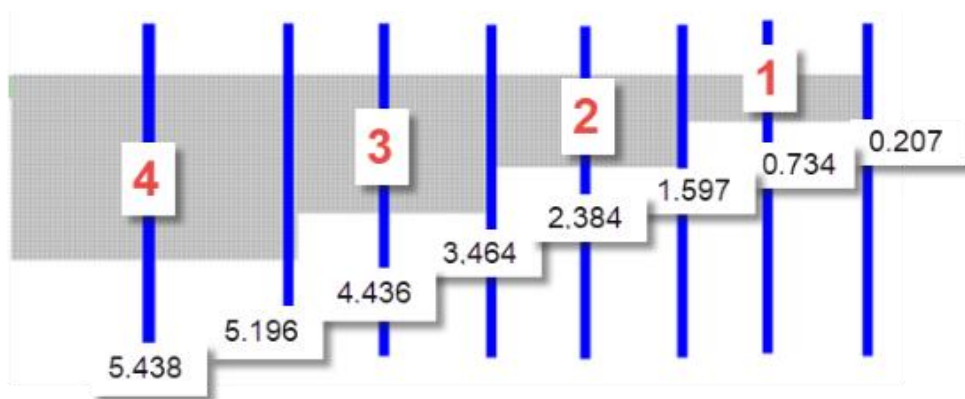


Fig. 4. Solidification time of the cast part given in minutes

### 3.2 Microstructural Studies

The microstructure pictures of the sample after polishing were taken at 50x magnification depending on the amount of inoculant at 0.06, 0.12, 0.24, and 0.3% levels which are given in Figure 5.

In the microstructural images given in Figure 5, it is understood that inoculation is effective in all of the cast samples. It is observed that casting graphite structures exhibit transformation from D-type

to A-type eutectic structures by the inoculation process [18]. As the inoculation content was increased, a greater number of graphites were formed in the structure, and the thickness and distribution of the graphites are appeared to be quite uniform. This is also consistent with studies conducted in the literature in which the formation of fine graphite flakes is a factor due to the fact that the number of nucleation was increased by the increased inoculant content [15]. It is also known that the inoculation process is important in terms of ensuring high lamellar numbers [12].

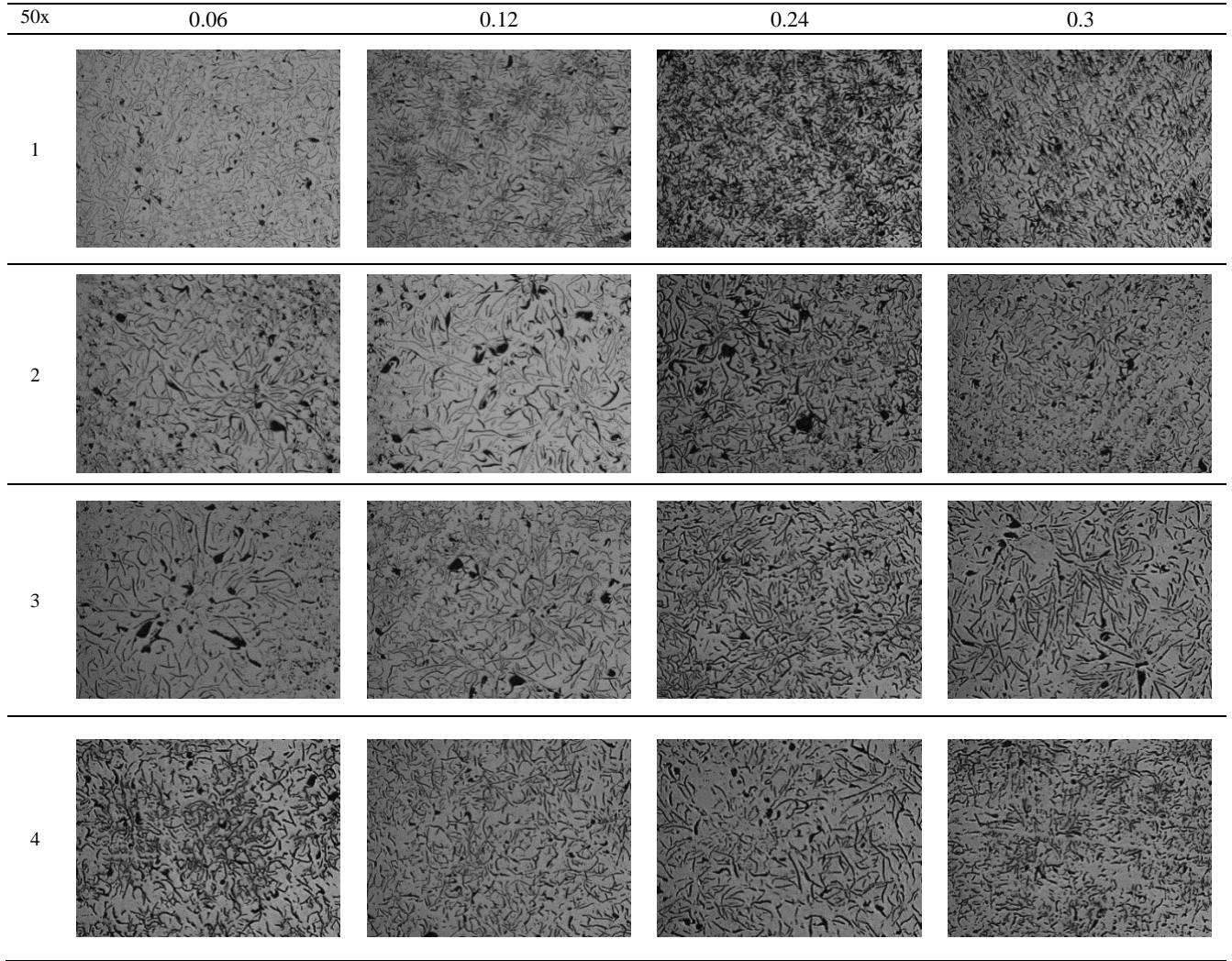


Fig. 5. Microstructure images of samples after polishing (50x)



If the effects of differences due to solidification time on the microstructure are examined, it is observed that graphite lamels appear in a thicker structure in the thickest section when solidification time is high. However, the difference in graphite thickening with regard to the solidification time is not very large which confirms the efficiency of the inoculation process in this case. This also confirms the fact that the inoculators are more effective when the cross-sectional thickness increases [28].

In Figure 6, the microstructure pictures taken from the samples produced with different amounts of inoculant at the 2nd region are given after etching. When the microstructure is examined, it is understood that it emerges as a ferritic and pearlitic structure around the lamellar graphite. It was determined that the structure consisted of the perlitic structure at 0.12 and more additional inoculation.

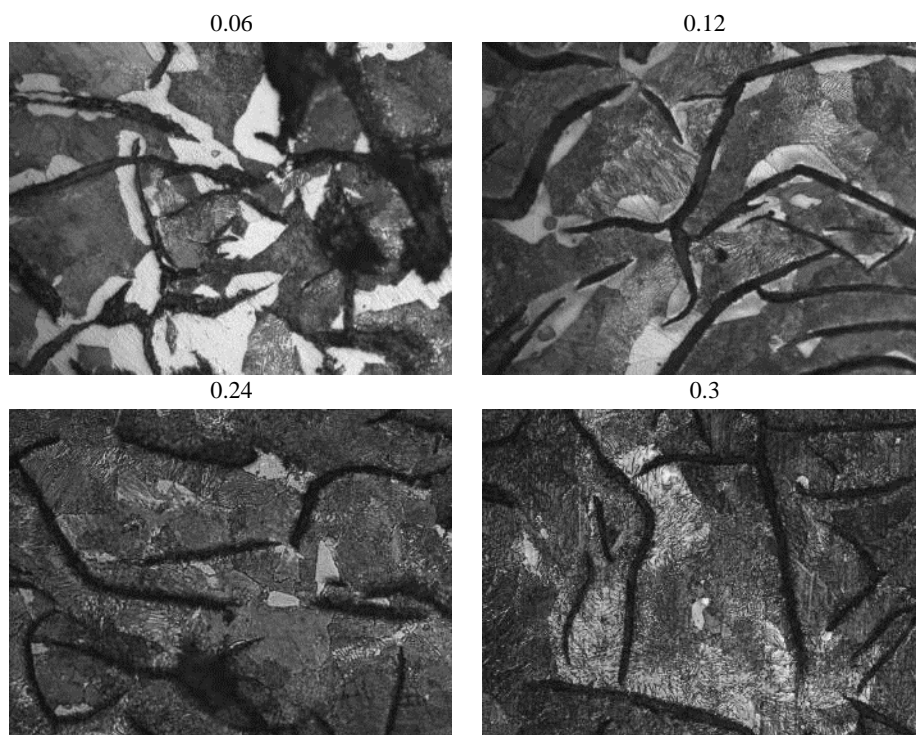


Fig. 6. Microstructure pictures of different inoculation amounts from region 2 (50x)

### 3.3 Image Analysis Results

Image analysis studies were performed with the help of Clemex Vision Lite software for each of the microstructure samples. In the image analysis evaluations performed after polishing, the average

length values, average thickness values, % graphite, and % main matrix ratios of the graphites found in the samples were determined, and the results were evaluated. Figure 7 shows a sample image of the processed image taken from the image analysis software.

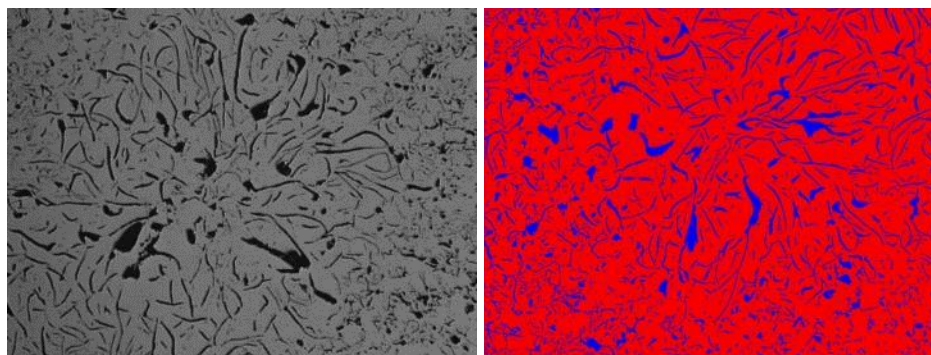


Fig. 7. Example of the processed image from the image analysis software

Average values of the results obtained from the software are given in Figures 8 and 9. It can be seen that the graphite thickness is varying between 20-38  $\mu\text{m}$  (Fig 8a). As the section thickness was increased, the graphite thickness was increased almost linearly. However, the change in the thickness was almost the same when 0.12, 0.24, and 0.3% inoculant were added. It appears that 0.12% is the critical limit above which the graphite thickness is not changed. A similar scenario applies to graphite length as well. As

seen in Figure 8b, the graphite length is increased linearly as the section thickness is increased. As the inoculant additions were higher than 0.24%, the graphite length is no longer affected by the inoculant amount. On the other hand, graphite ratio change with section thickness and inoculant amount reveals no clear relationship as can be seen in Figure 8c.

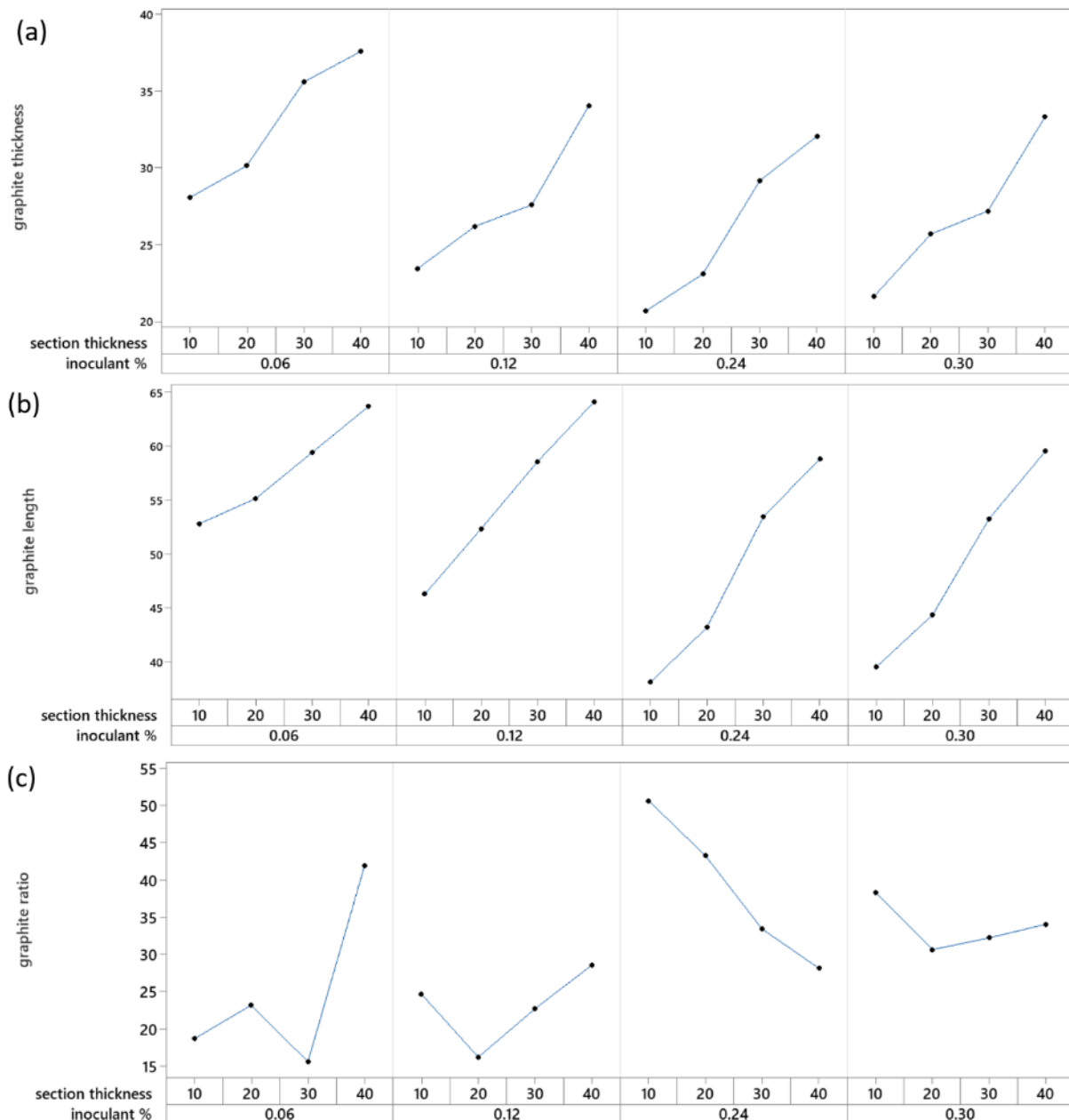


Fig. 8. (a) Graphite thickness with inoculant ratio and section thickness (b) Graphite length with inoculant ratio and section thickness (c) Graphite ratio with inoculant ratio and section thickness

Based on the data obtained from the image analysis and Figure 8, the main effect plots were drawn which can be seen in Figure 9. Section thickness has a clear effect on graphite thickness and

graphite length whereas the critical amount of inoculant appears to be 0.12% for graphite thickness and 0.24% for graphite length above which the values do not change [14].

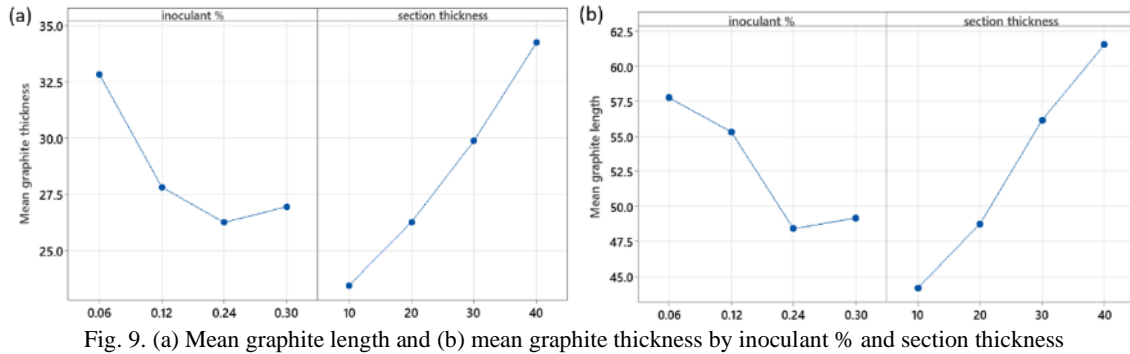


Fig. 9. (a) Mean graphite length and (b) mean graphite thickness by inoculant % and section thickness

When the results given in the table are examined, it is understood that the inoculant level of 0.06% and 0.12 is insufficient, and the inoculant level of 0.24 and 0.3 produces more suitable results in terms of length and thickness. It was determined that the graphite length and thickness increased from thin section to thick section depending on the section thickness. It is known that the number of graphite increases as reported in many studies due to the increase in the amount of inoculant [14, 24-27].

### 3.4. Hardness Tests

The hardness measurement results obtained from the test samples at different section thickness is given in Figure 10 with regard to the inoculant amount.

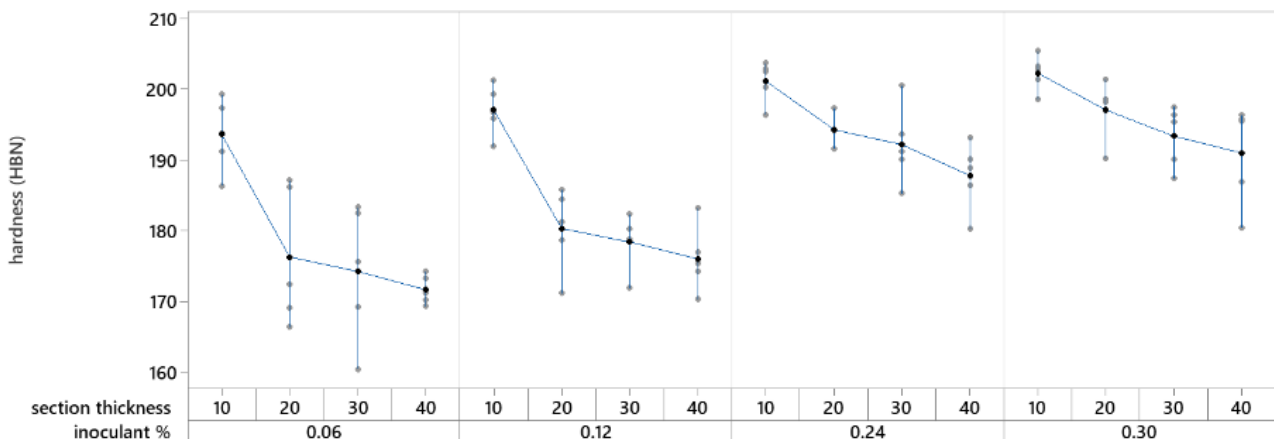


Fig. 10. Hardness measurement results

As can be seen from the results, the hardness values of the alloy studied in this work are among the standard values. In addition, depending on the change in solidification time (i.e. increased thickness), a decrease in the hardness values was detected with regard to increased section thickness. In addition, a slight increase in hardness values was detected due to the increase in the amount of inoculation. In a study in which the effect of the change in the amount of inoculation on the hardness change in spheroidal graphite cast iron was investigated, a decrease in the hardness ratio was found with the increase in the amount of inoculant addition [29].

## 4. Conclusions

Within the scope of the study, castings at different inoculation amounts were carried out in a design with varying section thicknesses. Microstructure pictures were taken from the samples obtained from the castings after polishing and after etching, and the images were evaluated by the image analysis. In addition, the hardness changes were investigated. The results obtained are as follows:

- Depending on the section thicknesses, changes were observed in the length and thickness of the graphite in the



microstructure. It was observed that the graphite thickness and length were increasing section thickness (i.e. slower cooling)

- For the effect of different amounts of inoculation additions, it is understood that the most appropriate inoculation amount in all sections is 0.24%. It is seen that 0.06% inoculation amount is insufficient, 0.12% inoculation amount is at an acceptable level. Since the inoculation amount at the level of 0.3% does not provide many advantages, it was considered unnecessary.
- In the microstructures examined after the etching, it was determined that the structure was pearlitic in all the additions above 0.12%, except 0.06%.
- When the hardness change was examined, the hardness values increased as the amount of inoculation increased; while the hardness value was 193.58 HBN in the thinnest section with 0.06% inoculation addition, the maximum hardness value was 202.26 HBN at 0.3% addition amount due to the increase in the amount of inoculation.
- When the hardness values depending on the solidification time were examined, the highest hardness values were determined in the thinnest sections similarly in all inoculation amounts. With the increase in the thickness of the section, the hardness values decreased in the sections with increasing solidification time.
- It has been determined that the two-stage addition method of inoculation (from the furnace to the ladle and from the ladle to the mold) applied was suitable for the design used in this work.
- It has been found that 0.24% inoculant addition is appropriate for the optimum casting structure, depending on the different solidification times depending on the different section thicknesses. It is thought that it will be possible to reach the target structure and properties by increasing the amount of inoculation for the parts with a much larger solidification time difference.

## Conflict of interest

All authors declare that they have no conflict of interest.

## References

- [1] Campbell, J. (2003). *Castings*. Second Edition. UK: University of Birmingham.
- [2] Fredriksson, H., Stjern Dahl, A. & Tinoco, J. (2005). On the solidification of nodular cast iron and its relation to the expansion and contraction. *Materials Science and Engineering A*. 413-414, 363-372. DOI: 10.1016/j.msea.2005.09.028.
- [3] Stefanescu, D.M. (1988). ASM Handbook Metals Handbook, Vol.15, Casting. ASM International, Metals Park, 296-307.
- [4] Theuvsen, K., Lacaze, J. & Laffont, L. (2016). Structure of graphite precipitates in cast iron. *Carbon*. 96, 1120-1128. <https://doi.org/10.1016/j.carbon.2015.10.066>.
- [5] Alonso, G., Stefanescu, D.M., Suarez, R., Loizaga, A. & Zarrabeitia, G. (2014). Kinetics of graphite expansion during eutectic solidification of cast iron. *International Journal of Cast Metals Research*. 27(2), 87-100. <https://doi.org/10.1179/1743133613Y.0000000085>.
- [6] Hellstrom, K., Dioszegi, A. & Diaconu, L. (2017). A broad literature review of density measurements of liquid cast iron. *Metals*. 7(5), 165, 1-20. <https://doi.org/10.3390/met7050165>.
- [7] Skaland, T., Grong, O. & Grong, T. (1993). A model for the graphite formation in ductile cast iron: Part I. Inoculation mechanisms. *Metallurgical and Materials Transactions A*. 24A, 2321-2345. <https://doi.org/10.1007/BF02648605>.
- [8] Stefanescu, D.M., Alonso, G. & Suarez, R. (2020). Recent developments in understanding nucleation and crystallization of spheroidal graphite in iron-carbon-silicon alloys. *Metals*. 10(2), 221, 1-39. <https://doi.org/10.3390/met10020221>
- [9] Rowley, T.M. (1993). *International atlas of casting defects*. Schaumburg, IL.
- [10] Zhang, Z., Flower, H.M. & Niu, Y.Z. (1989). Classification of degenerate graphite and its formation processes in heavy section ductile iron. *Materials Science and Technology*. 5(7), 657-664. <https://doi.org/10.1179/mst.1989.5.7.657>.
- [11] Ferro, P., Fabrizi, A., Cervo, R. & Carollo, C. (2013). Effect of inoculant containing rare earth metals and bismuth on microstructure and mechanical properties of heavy section near-eutectic ductile iron castings. *Journal of Materials Processing Technology*. 213, 1601-1608. <https://doi.org/10.1016/j.jmatprotec.2013.03.012>.
- [12] Skaland, T. (2003). A new method for chill and shrinkage control in ladle treated ductile iron. Keith Millis Symp. Ductile Cast Iron.
- [13] Borsato, T., Ferro, P., Berto, F. & Carollo, C. (2017). Mechanical and fatigue properties of pearlitic ductile iron castings characterized by long solidification times. *Engineering Failure Analysis*. 79, 902-912. <https://doi.org/10.1016/j.engfailanal.2017.06.007>.
- [14] Çolak, M. & Kaya, S. (2021). Investigation of the effect of inoculant and casting temperature on fluidity properties in the production of spheroidal graphite cast iron. *Transactions of the Indian Institute of Metals*. 74(2), 205-214. DOI: 10.1007/s12666-020-02159-5.
- [15] Skaland, T. (2005). *Nucleation mechanisms in ductile iron, Elkem foundry products*. Norway: Kristiansand.
- [16] Gobinath, V.M. & Annamalai, K. (2017). Effect of inoculation in chilled cast iron with different chill. *Materials Today: Proceedings*. 4(10), 10863-10869. <https://doi.org/10.1016/j.matpr.2017.08.040>.
- [17] Seidu, S.O. & Ripoşan, I. (2011). Thermal analysis of inoculated ductile irons. *UPB Scientific Bulletin Series B*. 3/2. 73(2), 241-254. ISSN 1454-2331.
- [18] Fraš, E. & Górný, M. (2012). Inoculation effects on cast iron. *Archives of Foundry Engineering*. 12(4), 39-46. DOI: 10.2478/v10266-012-0104-z.
- [19] Fraš, E. & Lopez, H. (1994). Generation of inner pressure during solidification of eutectic cast iron. *AFS Transactions*. 102, 597-601.
- [20] Nastac, L. & Stefanescu, D.M. (1995). Forecast of grey-to-white transition in cast iron by solidification modeling. *AFS Transaction*. 103, 329-337.
- [21] Fraš, E. & Górný, M. (2010). Mechanism of carbon influence on the transition from graphite to cementite eutectic in cast

- iron. *Archives of Foundry Engineering*. 10(2), 51-56. ISSN (1897-3310).
- [22] Effects of manganese in nodular (SG) iron, BCIRA Broadsheet, 2006, 211.
- [23] Koch, M., Soulas, K. (2014). Inoculation of grey and ductile iron. 7<sup>th</sup> International Ankiros Casting Congress, September 12-13, Istanbul, Turkey.
- [24] Webster, P.D. (1980). Fundamentals of foundry technology. First Published, Portcullis Press Ltd., 246-252.
- [25] Jain, P.L. (1992). Principles of foundry technology. Second Edition. New Delhi: Tata McGraw-Hill Publishing Company Ltd., 184-188.
- [26] Ductile Iron Molten Metal Processing. (1986). AFS Publication, 2<sup>nd</sup> Edition.
- [27] Quality Control Committee Cast Iron Division, factors affecting ductile iron nodule count: a literature review, AFS Transactions, 1993, 93(224), 1031-1097.
- [28] Heine, R.W. (1993). Nodule count: the benchmark of ductile iron solidification. *AFS Transactions*. 93(84), 879-884.
- [29] Karadeniz, E., Çolak, M. & Barutçu, F. (2017). Investigation of the effect of inoculant type and amount on microstructure and mechanical properties in the production of GGG-60 spheroidal graphite cast iron. *Omer Halisdemir University Journal of Engineering Sciences*. 6(1), 275-282. (in Turkish)
- [30] Çolak, M., Arslan, İ. & Gavgali, E. (2018). Solidification modeling of gray cast irons and comparison with real castings. *Engineering Sciences (NWSAENS)*. 13(4), 280-290. (in Turkish) <http://dx.doi.org/10.12739/NWSA.2018.13.4.1A0419>